THAT'S NO OCEAN MOON: EFFECTS OF TRANSIENT OBLIQUITY TIDAL HEATING IN MIMAS' WARM ICY INTERIOR PRESERVED AS A COLD FOSSIL FIGURE. S. Gyalay[1] and F. Nimmo[1], [1]University of California, Santa Cruz (UCSC; Santa Cruz, CA 95060, USA; sgyalay@ucsc.edu).

Mimas as a Potential Ocean Moon: Like his more-famous brother, Enceladus, the icy satellite Mimas has a very elliptical orbit around Saturn (eccentricities 0.0047 and 0.0196, respectively). Further, the two moons have similar sizes and semi-major axes; both exhibit an anomalously high libration—potential evidence for a global subsurface ocean [1, cf. 2]. Yet while Enceladus experiences cryo-volcanism and resurfacing, Mimas appears geologically inert despite its circumstances.

However, [3] have recently shown that tidal heat within Mimas may be capable of maintaining a global, sub-surface ocean *without* relaxing craters on its surface. Further, the impact that created Mimas' largest crater, Herschel, could have occurred without cracking through Mimas' ice shell [4]. But if such an ocean exists, it is unlikely to be long-lived as the tidal dissipation needed to maintain it would quickly circularize Mimas' orbit [e.g. 5], and Mimas' eccentricity is not currently being excited.

With evidence for a Mimatean ocean circumstantial at best, only a look inside Mimas can truly answer this question. Unfortunately, there is no gravity data for Mimas [cf. 6]. In recently accepted work [7] however, we argue that spatial variations in tidal heating within icy satellites such as Mimas may manifest in the moon's global shape. As the tidal heat distribution is sensitive to the moon's interior structure [e.g. 8, 9], we can infer Mimas' interior structure from its external shape. We outline the method below.

Inferring Mimas' Interior from its Exterior:

Internal structure controls tidal heat distribution. As a synchronous satellite orbits its host planet, differences in the planet's gravitational pull at either end of the satellite will stretch it. If the satellite has any eccentricity (ellipticity) or obliquity (tilt of the satellite's equator relative to its orbital plane), this tidal bulge will migrate across the satellite's surface to the part of the surface closest (and furthest) to the planet. The oscillation of the tidal bulge creates a characteristic tidal heating pattern, wherein friction within specific regions of the satellite generate great heat. This exact pattern depends on the interior structure, such as the thickness and depth of the tidal-heat-producing regions (typically the ice shell for an icy satellite), as well whether the material underlying the heat-producing region is rigid or fluid.

[9] has demonstrated that any tidal heating distribution can be represented by the linear combination of three basis heating patterns. With a multilinear regression, we can determine if an arbitrary heating pattern can be characterized as tidal heating, as well as calculate the exact weight of each basis pattern. We can thus infer the interior structure of a satellite from its tidal heating distribution.

Variations in tidal heat create long-wavelength topography. Here, we make the key assumption that Mimas' ice shell is in isostatic equilibrium—the principle that mass or pressure is constant at some depth [e.g. 10, cf. 11]. In an Airy isostasy case, topography is caused by thickness variations in the ice shell, but requires some less-rigid, denser material to compensate in thinner regions. For an icy satellite, this is often assumed to be a liquid water ocean. If the base of the ice shell is at a constant (melting) temperature globally, the heat flux through the ice shell—and thus the tidal heat producing it—can be calculated with Fourier's law of thermal conduction.

Alternatively in Pratt isostasy, topography arises from variations in density, i.e., thicker portions of the ice shell have a lower density and thinner portions have higher density. We assume that these density variations are caused by thermal expansion or contraction—calculating the necessary tidal heat production accordingly.

Altogether. Mimas' global shape (or, long-wavelength topography [12]) betrays variations in ice shell heating. We check if that heating is due to tides and what interior it suggests. This requires us to assume Mimas' moment of inertia (which controls a large contribution to long-wavelength topography [13]), a type of isostasy, eccentricity vs. obliquity tides, ice shell thickness, and how porous the upper ice shell (temperature <140 K [e.g. 14]) may be. We check for self-consistency between each set of assumptions and its inferred interior, e.g. whether such an interior is compatible with the assumed moment of inertia, or if topography forward-modeled from the fitted heating pattern weights agrees with Mimas' observed topography. Having tested this on Enceladus and Tethys [7], we turn our gaze to Mimas.

Results: We found no successful models that assumed Pratt isostasy. This leaves Airy isostasy models, implying Mimas' ice shell lies atop a denser, more-fluid layer. Further, any models that assumed eccentricity tides had a high misfit between Mimas' observed topography and forward-modeled topography from our inferred heating pattern. This leaves obliquity

tides, indicating that the tidal heating that formed Mimas' shape was due to a high tilt but little-to-no eccentricity.

In Figure 1 we examine the misfit of forward-modeled topography for Mimas models that assumed Airy isostasy and obliquity tides. The most self-consistent models indicate Mimas has a ~30 km thick ice shell and an average surface heat flow of 20 mW/m^2, for a total power of 10 GW.

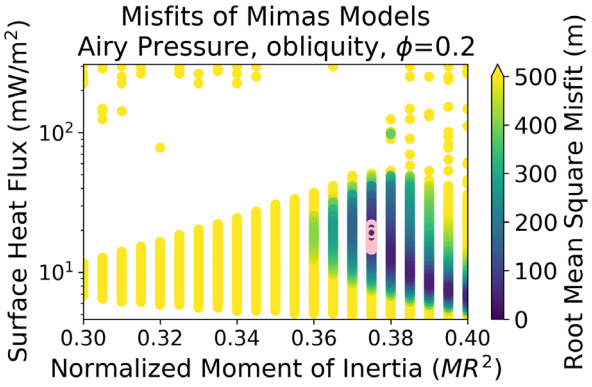

Figure 1: Misfit between observed topography and that forward-modeled from Mimas' inferred tidal heating pattern. All models here assumed equal-pressure Airy isostasy [e.g. 10], obliquity tides, and upper ice shell porosity φ=0.2. Surface heat flux depends on the ice shell's assumed thickness and basal temperature. Models circled in pink have the greatest self-consistency between assumed and inferred values.

Our inferred heat pattern for Mimas indicates tidal heating in a 66-km-thick ice shell over a more-rigid material (as opposed to less-rigid, as implied by the assumption of Airy isostasy) but also that at least half of Mimas' heat is produced in its core. As the low density of Mimas (1148 kg/m^3) precludes significant radiogenic heat in the core, it is more likely the core was itself tidally heated.

Conclusions: The discrepancy between an assumed 30 km ice shell over a more-fluid, denser layer, and the inferred tidal heating pattern of a 66 km ice shell over a rigid layer is resolved if the region of the ice shell 30-66 km deep is a convecting ice-rock mixture. When warm, such a mixture will be sufficiently ductile for the colder conductive ice shell above to experience Airy isostasy, while still being less rigid than the colder core beneath it. Further, the ice-rock layer will produce tidal heating commensurate with a 66 km thick ice shell [cf. 15]. With its thickness, the region's Rayleigh number is 100x greater than the critical value for (perhaps weak) convection. Using a numerical solid body tidal heating model [16, modified to include obliquity tides], we can reproduce the combined heating pattern of concurrent shell and core heating with our inferred Mimatean interior. However, this interior model with Mimas' present-day eccentricity would produce far greater heating with eccentricity tides.

This implies that the observed global shape of Mimas is a fossil figure: when the obliquity required to produce this amount of tidal heating (~2°) damped, Mimas quickly cooled and froze in this shape. Only later, when it was far more rigid and viscous, could it have gained its present-day eccentricity. Because a satellite's obliquity tends to trend toward the value of its inclination (angle between a satellite's orbital plane and the planet's equatorial plane), we speculate that Mimas' inclination (and thus obliquity) was temporarily excited 100s of Myr ago (if not more) as it passed through a past inclination-type resonance on its way to the present inclination-type resonance with Tethys [17-19]. Alternatively, close passage of a destabilized satellite which ultimately went on to form Saturn's rings 100-200 Ma [20] may have excited Mimas's inclination.

Regarding eccentricity, we estimate a slow (0.2 km/s) and large (~1% Mimas' mass) impactor may have excited Mimas eccentricity while forming Herschel crater [cf. 21]. The Herschel-forming impact is estimated to have occurred <1 Ga, perhaps even <100 Ma [22, 23; cf. 24, 25], and thus very well could have excited Mimas' eccentricity after Mimas damped the transiently high obliquity that carved its global shape.

References: [1] Tajeddine et al. (2014), *Sci. 346*(6207), 322. [2] Thomas et al. (2016), *Icarus 264*, 37. [3] Rhoden & Walker (2022), *Icarus 376*. [4] Denton & Rhoden (2022), *GRL 49*(24). [5] Noyelles et al. (2019), *Mon. Not. RAS 486*(2), 2947. [6] Iess et al. (2014), *Sci. 344*(6179), 78. [7] Gyalay & Nimmo (2023), *JGR: Planets*, in press (preprint). [8] Segatz et al. (1988), *Icarus 75*(2), 187. [9] Beuthe (2013), *Icarus 223*(1), 308. [10] Hemingway & Matsuyama (2017), *GRL 44*(15). [11] Beuthe (2021), *GJI 225*(3), 2157. [12] Nimmo et al. (2011), *JGR: Planets 116*(E11). [13] Beuthe et al. (2016), *GRL 43*(19), 10088. [14] Besserer et al. (2013), *JGR: Planets 118*(5), 908. [15] Roberts (2015), *Icarus 258*, 54. [16] Roberts & Nimmo (2008), *Icarus 194*(2), 675. [17] Sinclair (1983), *IAU Colloq. 74*, 19. [18] Vienne et al. (1996), *Sympos. IAU 172*, 143. [19] Champenoise & Vienne (1999), *Icarus 140*(1), 106. [20] Wisdom et al. (2022), *Sci. 377*(6612), 1285. [21] Zhang & Nimmo (2012), *Icarus 218*(1), 348. [22] Kirchoff & Schenk (2008), *Early Sol. Sys. Imp. Bombard.*, Abs. 3023, LPI Cont. 1439. [23] Kirchoff et al. (2018), *Enceladus and the Icy Moons of Saturn*, 267. [24] Ferguson et al. (2022a), *JGR: Planets 127*(6) [25] Ferguson et al. (2022b), *EPSL 593*.